

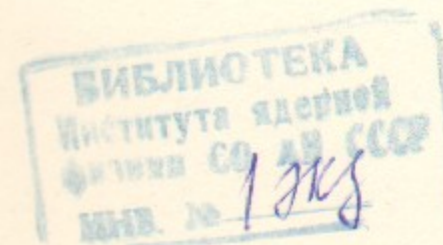


T.33
1998

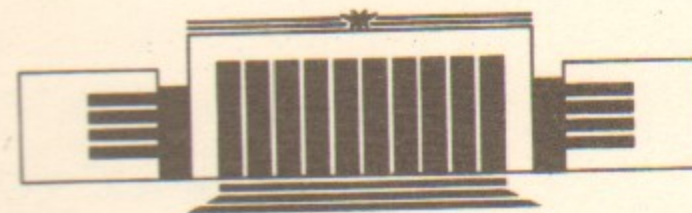
The State Scientific Center of Russia
The Budker Institute of Nuclear Physics
SB RAS

V.I. Telnov

ULTIMATE LIMINOSITIES AND ENERGIES
OF PHOTON COLLIDERS



Budker INP 97-47



НОВОСИБИРСК

✓

Ultimate luminosities and energies of photon colliders ¹

V.I. Telnov

Budker Institute of Nuclear Physics SB RAS
630090 Novosibirsk, Russia

Abstract

A photon collider luminosity and its energy are determined by the parameters of an electron-electron linear collider (energy, power, beam emittances) and collision effects. The main collision effect is the coherent e^+e^- pair creation. At low energies ($2E < 0.5-1$ TeV) this process is suppressed due to repulsion of electron beams. In this region $L_{\gamma\gamma}(z > 0.65) \geq 10^{35} \text{ cm}^{-2} \text{ s}^{-1}$ is possible ($10^{33} - 10^{34}$ is sufficient). At higher energies the limited average beam power and coherent pair creation restrict the maximum energy of photon colliders (with sufficient luminosity) at $E_{cm} \sim 5$ TeV. Obtaining high luminosities requires the development of new methods of production beams with low emittances such as a laser cooling.

©Budker Institute of Nuclear Physics SB RAS

¹Talk at the Int.Symp. on Future High Energy Colliders, ITP, UCSB, Santa Barbara, October 21-25, 1996

1 Introduction

Linear colliders offer the unique opportunities to study $\gamma\gamma$, γe interactions. Using the laser backscattering method one can obtain $\gamma\gamma$ and γe colliding beams with an energy and luminosity comparable to that in e^+e^- collisions or even higher (due to the absence of some beam collision effects). This can be done with a relatively small incremental cost. The expected physics in these collisions is very rich and complementary to that in e^+e^- collisions. Some characteristic examples are:

- a $\gamma\gamma$ collider provides the unique opportunities to measure the two-photon decay width of the Higgs boson, and to search for relatively heavy Higgs states in the extended Higgs models such as MSSM;
- a $\gamma\gamma$ collider is an outstanding W factory, with a WW pair production cross section by a factor of 10-20 larger than that in e^+e^- and with a potential of producing $10^6 - 10^7$ W 's per year, allowing a precision study of the anomalous gauge boson interactions;

- a $\gamma\gamma$, γe collider is a remarkable tool for searching for new charged particles, such as supersymmetric particles, leptoquarks, excited states of electrons, etc., as in $\gamma\gamma$, γe collisions they are produced with cross sections larger than those in e^+e^- collisions;
- Charged supersymmetric particles with masses higher than the beam energy could be produced with a γe collider.

The general scheme of a photon collider is shown in Fig. 1.

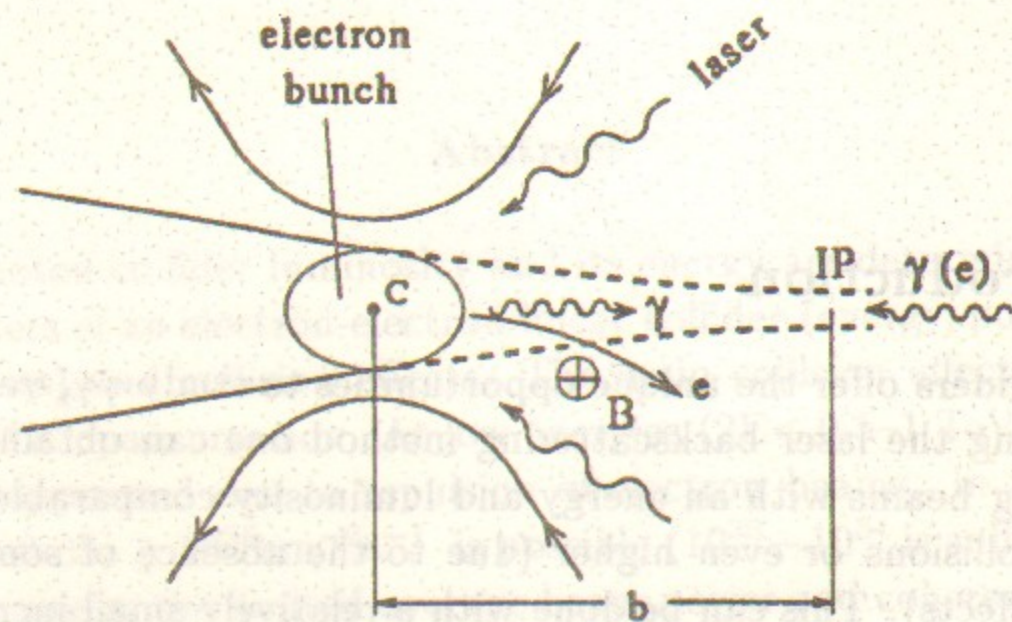


Figure 1: Scheme of $\gamma\gamma$; γe collider.

Two electron beams after the final focus system are traveling toward the interaction point (IP). At a distance of about 1 cm upstream from the IP, at a conversion point (CP), the laser beam is focused and Compton backscattered by the electrons, resulting in the high energy beam of photons. With reasonable laser parameters one can “convert” most of electrons to high energy photons. The photon beam follows the original electron direction of motion with a small angular spread of order $1/\gamma$, arriving at the IP in a tight focus, where it collides with a similar opposing high energy photon beam or with an electron beam. The photon spot size at the IP may be almost equal to that of electrons at IP and therefore the luminosity of $\gamma\gamma$, γe collisions will be of the same order as the “geometric” luminosity of basic ee beams.

The energy spectrum of photons after the Compton scattering for various polarization of electrons and laser photons is shown in fig. 2. At the optimum laser wave length (below the threshold of e^+e^- pair creation), the maximum energy of scattered photons is about 82% of the initial electron energy. Photons in the high energy part of spectrum can have high degree of polarization. This part of spectrum is most valuable for experiment. Below we will deal mainly with $\gamma\gamma$ luminosity produced by high energy photons.

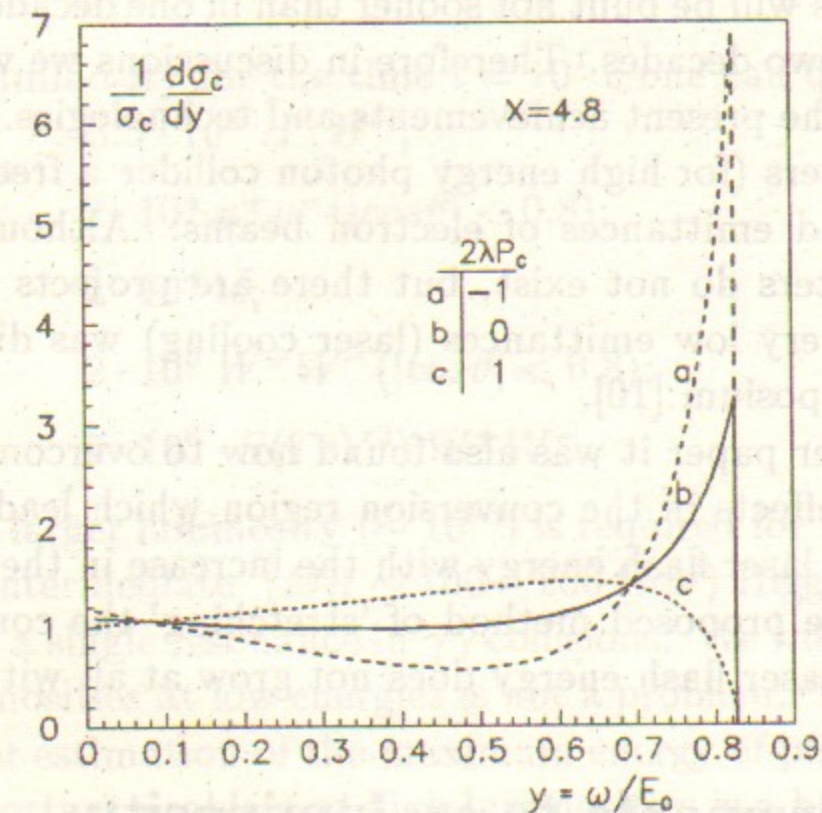


Figure 2: Spectrum of the Compton scattered photons for different polarizations of laser and electron beams

Here we will not consider the general features of photon colliders, they are described in papers [2]–[5] and Proceedings of the Berkeley Workshop [6].

Preliminary studies show that the photon colliders with an energy $2E \sim 500$ GeV and acceptable luminosity $L_{\gamma\gamma} \sim 10^{33} \text{ cm}^{-2} \text{ s}^{-1}$ (at $z = W_{\gamma\gamma}/2E > 0.7$) can be built [6, 1, 9]. However, physicists will be happy to have larger luminosity to study details of some processes, for example $\gamma\gamma \rightarrow \text{Higgs}$. It is also of interest to investigate main properties of the photon colliders at higher energy. We know that e^+e^- linear colliders at an energy above 1–2 TeV have serious problems. Is it easier to explore this region with a photon collider?

The present paper is focused mainly on the study of limitations on the energy and luminosity of photon colliders. We understand that linear colliders will be built not sooner than in one decade and will work another one–two decades. Therefore in discussions we will not confine ourselves by the present achievements and technologies. This concerns laser parameters (for high energy photon collider a free electron laser is needed) and emittances of electron beams. Although FELs with close parameters do not exist, but there are projects of such lasers. The way to very low emittances (laser cooling) was discussed at the first ITP symposium [10].

In the later paper it was also found how to overcome the problem of nonlinear effects in the conversion region which leads to the linear growth of the laser flash energy with the increase in the electron beam energy. In the proposed method of ‘stretching’ the conversion region the required laser flash energy does not grow at all with energy.

2 Requirements to $\gamma\gamma$ luminosity

Cross sections of the charged particle production in $\gamma\gamma$ collisions are somewhat higher than those in e^+e^- collisions. At $E \gg Mc^2$ the ratio of cross sections are the following:

$$\begin{aligned} \sigma_{\gamma\gamma \rightarrow H^+H^-} / \sigma_{e^+e^- \rightarrow H^+H^-} &\sim 4.5; \\ \sigma_{\gamma\gamma \rightarrow t\bar{t}} / \sigma_{e^+e^- \rightarrow t\bar{t}} &\sim 4; \\ \sigma_{\gamma\gamma \rightarrow W^+W^-} / \sigma_{e^+e^- \rightarrow W^+W^-} (|\cos\vartheta| < 0.8) &\sim 15; \end{aligned}$$

$$\sigma_{\gamma\gamma \rightarrow \mu^+\mu^-} / \sigma_{e^+e^- \rightarrow \mu^+\mu^-} (|\cos\vartheta| < 0.8) \sim 8.5.$$

To have the same statistics (but complementary physics) in $\gamma\gamma$ collisions the luminosity can be smaller than that in e^+e^- collisions by a factor of 5.

Cross sections decrease usually as $1/S$ ($S = E_{cm}^2$), therefore the luminosity should grow proportionally to S . A reasonable scaling for the required $\gamma\gamma$ luminosity (in the high energy peak of the luminosity distribution) at $\gamma\gamma$ collider is

$$L_{\gamma\gamma} \sim 3 \cdot 10^{33} S, \text{ cm}^{-2} \text{ s}^{-1}. \quad (1)$$

With such a luminosity for the time $t = 10^7$ c one can detect

$$\begin{aligned} &3.5 \cdot 10^3 H^+H^-, \\ &2 \cdot 10^4 \mu^+\mu^- (|\cos\vartheta| < 0.8); \\ &2 \cdot 10^4 t\bar{t}; \\ &2 \cdot 10^5 W^+W^- (|\cos\vartheta| < 0.8); \\ &2 \cdot 10^6 \cdot S(\text{TeV}^2) W^+W^-. \end{aligned}$$

Somewhat larger luminosity ($\sim 10^{33}$) is required for the search and study of the ‘intermediate’ ($M_H \sim 100 - 200$ GeV) Higgs boson which is produced as a single resonance in $\gamma\gamma$ collisions. We will see that such a level of luminosities at low energies is not a problem. The scaling (1) will be used for estimation of the maximum energy of photon colliders.

Other important problem at high luminosities is a background due to large total cross section $\sigma_{\gamma\gamma \rightarrow \text{hadrons}} \sim 5 \cdot 10^{-31} \text{ cm}^{-2} \text{ s}^{-1}$. It consists of particles with $P_t \sim 0.5$ GeV uniformly (at large angles) distributed over the pseudorapidity $\eta = -\ln \tan(\vartheta/2)$ with $dN/d\eta \sim 7$ at $2E = 500$ GeV. Particle density grows only logarithmically with energy.

The average number of hadron events/per bunch crossing is about one at $L_{\gamma\gamma}(z > 0.65) = 10^{34} \text{ cm}^{-2} \text{ s}^{-1}$ and at the typical collision rate 5 kHz. In this paper, we are interested mainly by the luminosity in the high energy part of luminosity spectrum. However, in the scheme without deflection of used electron beams the total $\gamma\gamma$ luminosity is larger than the ‘useful’ $L_{\gamma\gamma}(z > 0.65)$ by a factor 5–10 due to collisions

of low energy Compton photons and beamstrahlung photons. This low energy collisions increase background by a factor 2-3. At $E_{cm} = 5$ TeV with required $L_{\gamma\gamma}(z > 0.65) \sim 10^{35}$, this leads to about 30 (effectively) high energy $\gamma\gamma \rightarrow hadron$ events per bunch crossing. Similar number of hadronic events/collision is expected at LHC. However, there is important an difference between pp and $\gamma\gamma$ colliders: in the case of an interesting event (high P_t jets and leptons) the total energy of final products at photon colliders is equal to E_{cm} , while at proton colliders it is only about $(1/6)E_{cm}$. The ratio of the signal to background at photon colliders is better by a factor 6 at the same number of hadronic events per crossing. Moreover, during the reconstruction of an interesting event one can subtract smooth hadronic background and only its fluctuations are important which are proportional to \sqrt{L} . It means that for $L \propto E^2$ (and fixed collision rate) the ratio of signal to background is almost constant (decreases only logarithmically).

The above arguments shows that the problem of hadronic background is not dramatic for photon colliders. Of course, some increase in the collision rate with an increase in the luminosity will be useful. We will see that due to collision effects the optimum number of particles in one bunch should decrease with energy, that naturally leads to an increase in the collision rate.

3 Collision effects. Coherent pair creation.

There are two basic collision schemes [5]:

Scheme A ("without deflection"). There is no magnetic deflection of the spent electrons and all particles after the conversion region travel to the IP. The conversion point may be situated very close to the IP.

Scheme B ("with deflection"). After the conversion region particles pass through a region with a transverse magnetic field where electrons are swept aside. Thereby, one can achieve a more or less pure $\gamma\gamma$ or γe collisions.

During beam collision, photons are influenced by the field of the opposing electron beam. One of the important processes in this field is a conversion of photons into e^+e^- pairs (coherent pair creation)[7].

Under a certain conditions, the conversion length is shorter than the length of interaction region ($\sim \sigma_z$) and $\gamma\gamma$ luminosity is suppressed.

The probability of pair creation per unit length by a photon with the energy ω in the magnetic field $B(|B| + |E|)$ for our case) is [7],[4],

$$\mu(\kappa) = \frac{\alpha^2}{r_e} \frac{B}{B_0} T(\kappa), \quad (2)$$

where $\kappa = \frac{\omega}{mc^2} \frac{B}{B_0}$, $B_0 = \frac{m^2 c^3}{e\hbar} = \frac{\alpha e}{r_e^2} = 4.4 \cdot 10^{13}$ G is the the critical field, $r_e = e^2/mc^2$ is the classical radius of electron.

$$T(\kappa) \approx 0.16\kappa^{-1} K_{1/3}^2(4/3\kappa) \quad (3)$$

$$\begin{aligned} &\approx 0.23 \exp(-8/3\kappa) && \kappa < 1 \\ &\approx 0.1 && \kappa = 3 - 100 \\ &\approx 0.38\kappa^{-1/3} && \kappa > 100 \end{aligned}$$

In our case, $\omega \sim E_0$, therefore one can put

$$\kappa \sim \Upsilon \equiv \gamma B/B_0. \quad (4)$$

The probability to create e^+e^- pair during the collision time is

$$p \approx \mu \sigma_z = \frac{\alpha^2 \sigma_z}{r_e \gamma} \Upsilon T(\Upsilon). \quad (5)$$

From these equations we can find Υ for a certain conversion probability p (with an accuracy higher than 25%)[4]

$$\Upsilon_m = 2.7/\ln(0.1/p_1) \quad p_1 < 0.01, \quad (6)$$

$$1.2 + 9p_1 \quad 0.01 < p_1 < 4,$$

$$4.5 p_1^{3/2} \quad p_1 > 4,$$

where

$$p_1 = p \frac{r_e \gamma}{\alpha^2 \sigma_z} \sim p \cdot 0.1 \frac{E[\text{TeV}]}{\sigma_z[\text{mm}]}$$

For the conversion probability p the 'geometrical' $\gamma\gamma$ luminosity is suppressed approximately by a factor e^{-p} .

We will see that maximum $\gamma\gamma$ luminosity is achieved at $p > 1$. For $E = 0.5 - 2.5$ TeV and $\sigma_z = 0.1 - 0.5$ mm the parameter p_1 belongs to the second range ('transition' regime) where $\Upsilon \sim 1.2 + 9p_1$.

4 Estimation of ultimate $\gamma\gamma$ luminosity

Let us find now limits posed on the luminosity due to coherent pair creation for different collision schemes.

There are three ways to avoid this effect (i.e. to keep $\Upsilon \leq \Upsilon_m$):

- 1) to use flat beams;
- 2) to deflect the electron beam after conversion at a sufficiently large distance (x_0 for $E = E_0$) from the interaction point (IP);
- 3) under certain conditions (low beam energy, long bunches) $\Upsilon < \Upsilon_m$ at the IP due to the repulsion of electron beams [8].

Let us consider at first requirements to the beam sizes in the case 1.

4.1 Flat beams

The field of the beam with the r.m.s horizontal size σ_x and the length σ_z is $B \equiv |B| + |E| \sim 2eN/\sigma_x\sigma_z$. From the condition $\kappa \sim 0.8\gamma B/B_0 < \Upsilon_m$ we get

$$\sigma_x > \frac{1.6N\gamma r_e^2}{\alpha\sigma_z\Upsilon_m} = \frac{1.6N\gamma r_e^2}{\alpha\sigma_z(1.2 + 9p r_e\gamma/\alpha^2\sigma_z)} \sim \frac{40 \cdot \left[\frac{N}{10^{10}}\right]}{p + 1.3\frac{\sigma_z[\text{mm}]}{E[\text{TeV}]}} \text{ nm} \quad (7)$$

The $\gamma\gamma$ luminosity at $z > 0.65$

$$L_{\gamma\gamma} \sim \frac{0.5k^2N^2f}{4\pi(b/\gamma)\sigma_x} \sim \frac{0.025\alpha N\sigma_zfk^2}{br_e^2} \left[1.2 + 9p\frac{r_e\gamma}{\alpha^2\sigma_z}\right] e^{-p}, \quad (8)$$

where the coefficient 0.5 follows from the simulation for $\sigma_y = b\gamma$. It has its maximum at

$$I: \quad \tilde{p} = 0 \quad \text{at} \quad a = \frac{7.5r_e\gamma}{\alpha^2\sigma_z} = \frac{0.75E[\text{TeV}]}{\sigma_z[\text{mm}]} < 1;$$

$$II: \quad \tilde{p} = 1 - 1/a \quad \text{at} \quad a > 1.$$

The corresponding luminosities for these two cases are the following

$$L_{\gamma\gamma} \sim 0.03 \frac{\alpha k^2 N f \sigma_z}{br_e^2} = 2.8 \cdot 10^{33} \left(\frac{N}{10^{10}}\right) \frac{f[\text{kHz}]}{b[\text{cm}]} k^2 \sigma_z[\text{mm}], \text{ cm}^{-2}\text{s}^{-1}; \quad (9)$$

$$L_{\gamma\gamma} \sim 0.23 \frac{N f \gamma k^2}{\alpha b r_e} e^{-\tilde{p}} = 2.2 \cdot 10^{33} \left(\frac{N}{10^{10}}\right) \frac{f[\text{kHz}]}{b[\text{cm}]} k^2 E[\text{TeV}] e^{-\tilde{p}}, \text{ cm}^{-2}\text{s}^{-1}. \quad (10)$$

Optimum horizontal beam sizes in these two cases are

$$I: \quad \sigma_x \sim \frac{1.3N r_e^2 \gamma}{\alpha \sigma_z} = 28 \frac{E[\text{TeV}] \left(\frac{N}{10^{10}}\right)}{\sigma_z[\text{mm}]}, \text{ nm}; \quad \text{at } a < 1; \quad (11)$$

$$II: \quad \sigma_x \sim 0.18\alpha N r_e = 37 \left(\frac{N}{10^{10}}\right), \text{ nm} \quad \text{at } a > 1. \quad (12)$$

The minimum value of the distance between the conversion (CP) and the interaction regions b is determined by the length of the conversion region which is equal approximately to $b = 0.08E[\text{TeV}]$, cm (see section 6.1). For further estimation we assume that

$$b = 3\sigma_z + 0.04E[\text{TeV}], \text{ cm}. \quad (13)$$

Let us take $N = 10^{10}$, $\sigma_z = 0.2$ mm, $f = 10$ kHz, $k^2 = 0.4$ (one conversion length) that corresponds at $E > 0.25$ TeV to the case II. For $2E = 5$ TeV we get

$$L_{\gamma\gamma} \sim 6 \cdot 10^{34} \text{ cm}^{-2}\text{s}^{-1} \quad \text{at } \sigma_x \sim 40 \text{ nm} \quad \text{and } \sigma_y \sim b/\gamma = 0.3 \text{ nm}. \quad (14)$$

For a very high energy $L_{max} \sim 8 \cdot 10^{34} \text{ cm}^{-2}\text{s}^{-1}$ for a chosen parameters corresponding to the beam power $P = 15E[\text{TeV}]$ MW per beam. In the next section we will compare these approximate results with the results of simulation.

4.2 Influence of the beam-beam repulsion on the coherent pair creation

During the beam collision electrons get displacement in the field of the opposing beam

$$r \sim \sqrt{\frac{\sigma_z r_e N}{8\gamma}} \quad (15)$$

This estimate is obtained from the condition that at the impact parameter equal to the characteristic displacement the additional displacement is equal to the initial impact parameter.

The field at the axis (which influences on the high energy photons) $B \sim 2eN/r\sigma_z$. Then the corresponding field parameter

$$\Upsilon \sim \gamma \frac{B}{B_0} = \frac{\gamma B r_e^2}{\alpha e} \sim 5 \frac{r_e \gamma}{\alpha \sigma_z} \sqrt{\frac{\gamma r_e N}{\sigma_z}} \quad (16)$$

According to eq.(6), in the transition regime $\Upsilon_m = 1.2 + 9pr_e\gamma/\alpha^2\sigma_z$. From $\Upsilon = \Upsilon_m$ we can find the maximum beam energy when the coherent pair creation is suppressed due to the beam repulsion.

At the energy $E > 1$ TeV and bunches short enough, one can neglect the first term and get

$$\gamma_{max} \sim 3 \frac{p^2 \sigma_z}{\alpha^2 r_e N} \quad \text{or} \quad E_{max} \sim p^2 \frac{\sigma_z [\text{mm}]}{N/10^{10}}, \text{ TeV} \quad (17)$$

The $\gamma\gamma$ luminosity is equal

$$L_{\gamma\gamma}(z > 0.65) \sim 0.35 \frac{N^2 f k^2}{4\pi (b/\gamma)^2} e^{-p} \sim 0.1 (Nf) \frac{\sigma_z \gamma p^2 k^2}{\alpha^2 r_e b^2} e^{-p}, \quad (18)$$

where the numerical factor 0.35 follows from the simulation. It has its maximum at $p=2$ when

$$L_{\gamma\gamma} \sim 0.05 (Nf) \frac{\sigma_z \gamma k^2}{\alpha^2 r_e b^2} \sim 7 \cdot 10^{33} \left(\frac{N}{10^{10}} \right) \frac{\sigma_z [\text{mm}]}{b^2 [\text{cm}]} E [\text{TeV}] f [\text{kHz}] k^2 \sigma_z [\text{mm}]. \quad (19)$$

We have separated the factor (Nf) because it is a beam power. Taking in the previous example $Nf = 10^{14}$ Hz, $\sigma_z = 0.2$ mm, $k^2 = 0.4$, $b = 3\sigma_z + 0.04E [\text{TeV}]$, cm, $E = 2.5$ TeV we obtain

$$L_{\gamma\gamma}(z > 0.65) \sim 6 \cdot 10^{35} \text{ cm}^{-2} \text{ s}^{-1}. \quad (20)$$

The optimum number of particles in the beam for an energy considered (eq.(17)) is $N \sim 0.8 \cdot 10^{10}$.

These estimates show that the beam repulsion substantially influences (increases) the attainable $\gamma\gamma$ luminosity. This prediction will be checked by the simulation.

In fact, at low enough energy this effect allows to use even infinitely narrow electron beams with any reasonable number of particles in the bunch and the minimum photon spot size is b/γ , where b should be taken as small as possible. At high energies this effect also works but the number of particles in the bunch should be below some number dependent of the energy (eq.17).

5 Scheme with magnetic deflection

Using the magnetic field B_e between the conversion and interaction regions one can sweep out electrons from the interaction point at some distance x_0 sufficient for the suppression of coherent pair creation, i.e. to satisfy condition $\Upsilon < \Upsilon_m$ given by eq.6. This distance x_0 is approximately equal to σ_x given by eq.7. The required distance b is found from relation $x_0 \sim b^2/2R = b^2 e B_e / 2E$. The photon spot size at IP is b/γ and the luminosity of $\gamma\gamma$ collisions

$$L_{\gamma\gamma}(z > 0.65) \sim 0.35 \frac{k^2 N^2 f}{4\pi (b/\gamma)^2} \sim \frac{0.03 \alpha k^2 N f \sigma_z B_e}{e r_e} \left(1 + 7.5 p \frac{r_e \gamma}{\alpha^2 \sigma_z} \right) e^{-p} \quad (21)$$

The optimization over p gives

$$L_{\gamma\gamma} \sim \frac{0.03 \alpha k^2 N f \sigma_z B_e}{e r_e} =$$

$$= 1.6 \cdot 10^{34} \left(\frac{N}{10^{10}} \right) \sigma_z [\text{mm}] f [\text{kHz}] B_e [\text{T}] k^2 \text{ at } a = \frac{0.75 E [\text{TeV}]}{\sigma_z [\text{mm}]} < 1; \quad (22)$$

$$L_{\gamma\gamma} \sim \frac{0.22 k^2 N f \gamma B_e}{\alpha e} e^{-(1-1/a)} =$$

$$= 1.25 \cdot 10^{34} \left(\frac{N}{10^{10}} \right) f [\text{kHz}] B [\text{T}] E [\text{TeV}] k^2 e^{-(1-1/a)}, \text{ cm}^{-2} \text{ s}^{-1}; \text{ at } a > 1. \quad (23)$$

As before, taking $N = 10^{10}$, $f = 10$ kHz, $\sigma_z = 0.2$ mm, $k^2 = 0.4$ $E = 2.5$ TeV and $B_e = 0.5$ T we get

$$L_{\gamma\gamma}(z > 0.65) \sim 2.5 \cdot 10^{34} \text{ cm}^{-2} \text{ s}^{-1}. \quad (24)$$

This number is notably smaller than that in the scheme without deflection eq(20). The luminosity is proportional to B_e and one can take larger field values but it poses some technical problems. One should also remember that in the transverse magnetic field, the soft background particles produced in the forward direction (mainly e^+e^- pairs) get a kick, begin to spiral in the detector field and to avoid backgrounds the radius of the vacuum pipe should exceed $r = 2bB_{\perp}/B_{\parallel}$.

Considering the scheme with deflection we did not consider the field created by the produced e^+e^- pairs. These particles are closer to the beam axis than the deflected beam and their field can even exceed the field of the opposing electron beam. Therefore, our optimization of pair creation overestimates the luminosity. We will see results of simulation in next sections.

6 Simulation

6.1 Assumptions

We have seen that the picture of collisions is very complicated. It is easier to get the result by simulation. The simulation code used in this work [5] includes all important processes. In the present study, the beams are collided in very ultimate conditions: very small beam

sizes, high energies, too many beamstrahlung photons. In order to avoid the time consumption problem only one simplification was done: charged particles emitted the beamstrahlung photons during the beam collision but these photons were excluded from further consideration. It was assumed that:

- the thickness of the laser target is equal to one collision length ($k = 1 - e^{-1} \sim 0.6$);
- electrons and laser photons are polarized and $2P_c \lambda_e = -1$;
- varying the number of particles in the beam we kept constant beam power $NfE = 15E[\text{TeV}]$, MW;
- the minimum distance between the CP and IP region was taken to be $b = 0.2 + 0.1E[\text{TeV}]$, cm for fig. 3 and $b = 3\sigma_z + 0.04E[\text{TeV}]$ cm for the rest figures. In the later case, the parameter ξ^2 characterizing the nonlinear effect in the Compton scattering [5] is equal to 0.6;
- the vertical beam size is equal to $0.5b/\gamma$;

6.2 Simulation results

Fig. 3 shows $\gamma\gamma$ luminosity as a function of σ_x at TESLA and NLC for the beam energy range 0.25–4 TeV. On the righthand graphs, the number of particles was decreased by a factor 10, while the collision rate was increased by the same factor. The distance $b = 0.2 + 0.1E[\text{TeV}]$ cm. We see on the left-hand side graphs that for 'nominal' numbers of particles in the beams the luminosity does not follow the dependence $L \propto 1/\sigma_x$ due to the conversion of photons to e^+e^- pairs. It happens at σ_x very close to our prediction, eq(12).

In fig. 4 we can see the dependence of the luminosity both on N and σ_z in the case where beams are round and the conversion region is situated as close as possible: $b = 3\sigma_z + 0.04E[\text{TeV}]$ cm. The total beam power is $15E[\text{TeV}]$ MW. Looking to this pictures one can make many own observations which are clear after our theoretical consideration. Note only that the longer bunch requires the larger laser flash energy for conversion ($A \propto \sigma_z$) and not every linac (among the current projects) can accelerate a 0.5 mm long bunch due to wake fields. Let us take for further study $\sigma_z = 0.2$ mm.

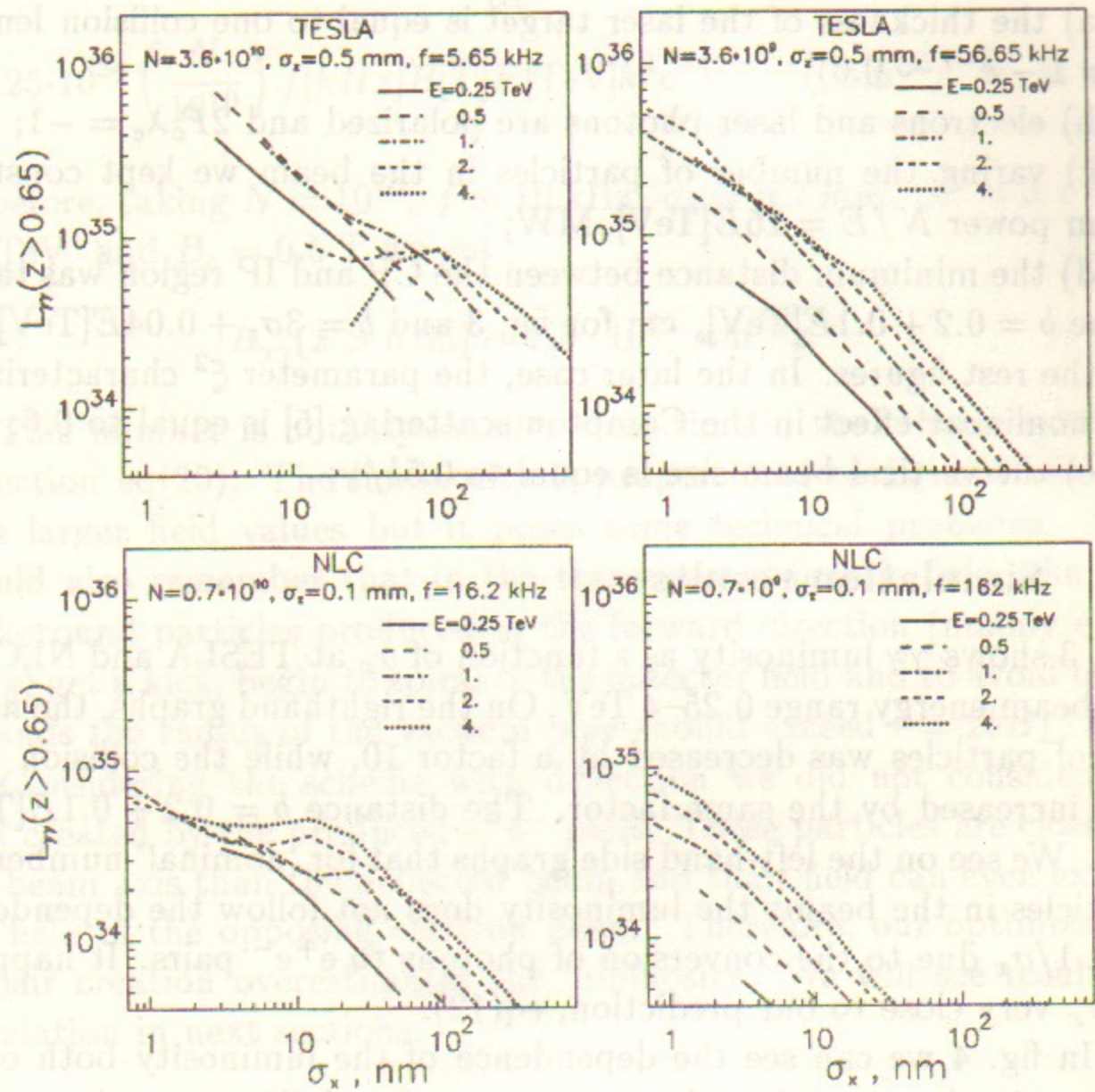


Figure 3: Dependence of the $\gamma\gamma$ luminosity on the horizontal beam size for TESLA and NLC beam parameters, see comments in the text.

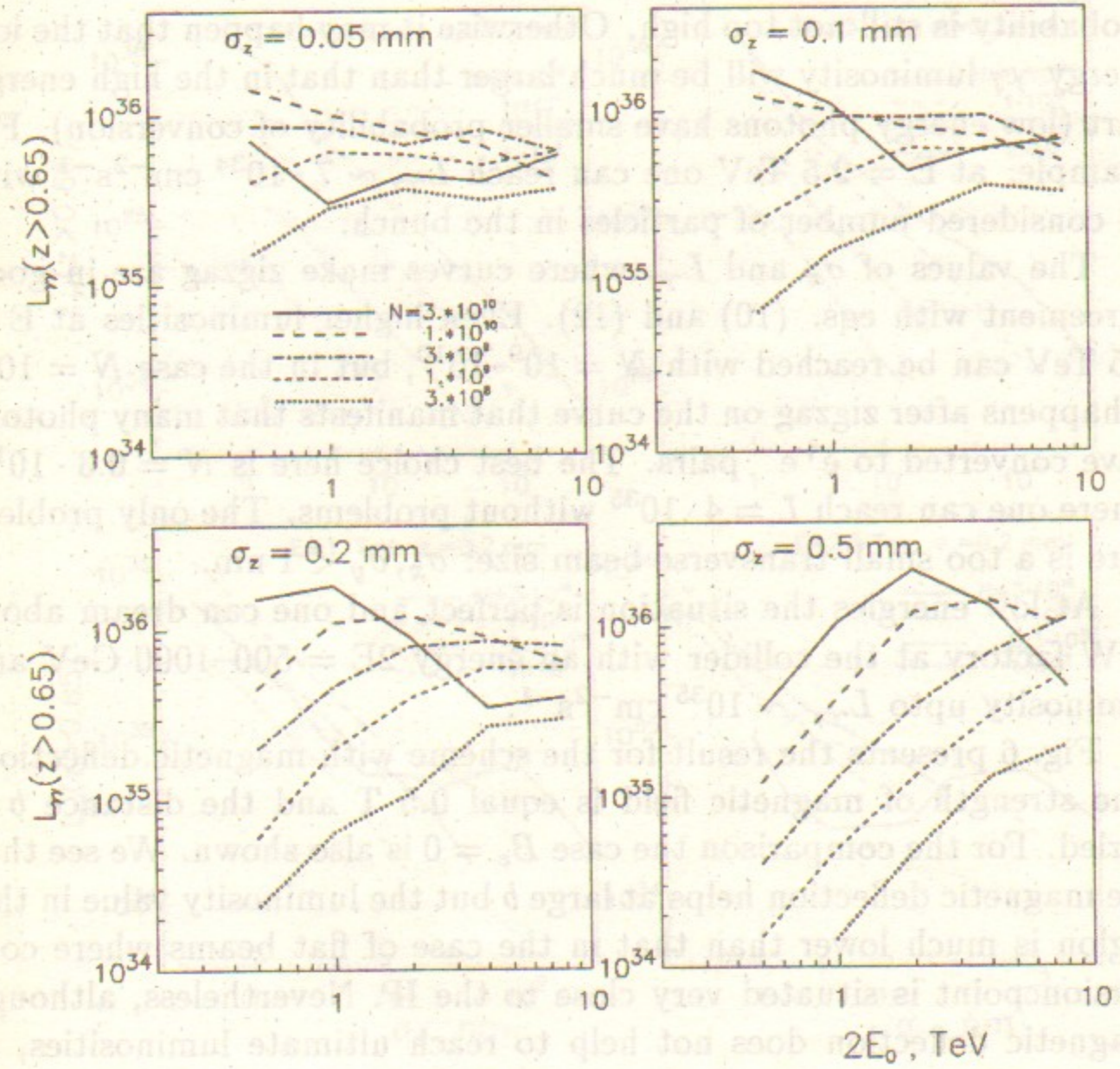


Figure 4: $\gamma\gamma$ luminosity for round beams at the minimum distance between interaction region and collision points, see comments in the text.

The dependence of the luminosity on σ_x (other conditions are the same as in the previous figure) is depicted in fig. 5. It is desirable to choose the working point (σ_x, N) so that not only the luminosity is large but also the corresponding curve still follows their natural behavior $L \propto 1/\sigma_x$. This means that the $\gamma \rightarrow e^+e^-$ conversion probability is still not too high. Otherwise it may happen that the low energy $\gamma\gamma$ luminosity will be much larger than that in the high energy part (low energy photons have smaller probability of conversion). For example: at $E = 2.5$ TeV one can reach $L_{\gamma\gamma} \sim 7 \cdot 10^{34} \text{ cm}^{-2}\text{s}^{-1}$ with all considered number of particles in the bunch.

The values of σ_x and $L_{\gamma\gamma}$ where curves make zigzag are in good agreement with eqs. (10) and (12). Even higher luminosities at $E = 2.5$ TeV can be reached with $N = 10^9 - 10^{10}$, but in the case $N = 10^{10}$ it happens after zigzag on the curve that manifests that many photons have converted to e^+e^- pairs. The best choice here is $N = 0.3 \cdot 10^{10}$, where one can reach $L = 4 \cdot 10^{35}$ without problems. The only problem here is a too small transverse beam size: $\sigma_x, \sigma_y < 1 \text{ nm}$.

At low energies the situation is perfect and one can dream about WW factory at the collider with an energy $2E = 500 - 1000 \text{ GeV}$ and luminosity upto $L_{\gamma\gamma} \sim 10^{35} \text{ cm}^{-2}\text{s}^{-1}$.

Fig. 6 presents the result for the scheme with magnetic deflection. The strength of magnetic field is equal 0.5 T and the distance b is varied. For the comparison the case $B_e = 0$ is also shown. We see that the magnetic deflection helps at large b but the luminosity value in this region is much lower than that in the case of flat beams where conversion point is situated very close to the IP. Nevertheless, although magnetic deflection does not help to reach ultimate luminosities, in 'practical' cases (where the luminosity is far from the limit) the magnetic deflection helps to decrease the low energy $\gamma\gamma$ luminosity without degradation of the high energy part.

Comparing our luminosity scaling law (eq.1) with the results of the simulation we see that the required luminosity can be reached at least up to $2E = 4 \text{ TeV}$ with any (up to $3 \cdot 10^{10}$) number of particles in the bunch. Note that in our examples the collision rate is $f = 10 \text{ kHz}(10^{10}/N)$. The higher f is good for the experiment but makes some

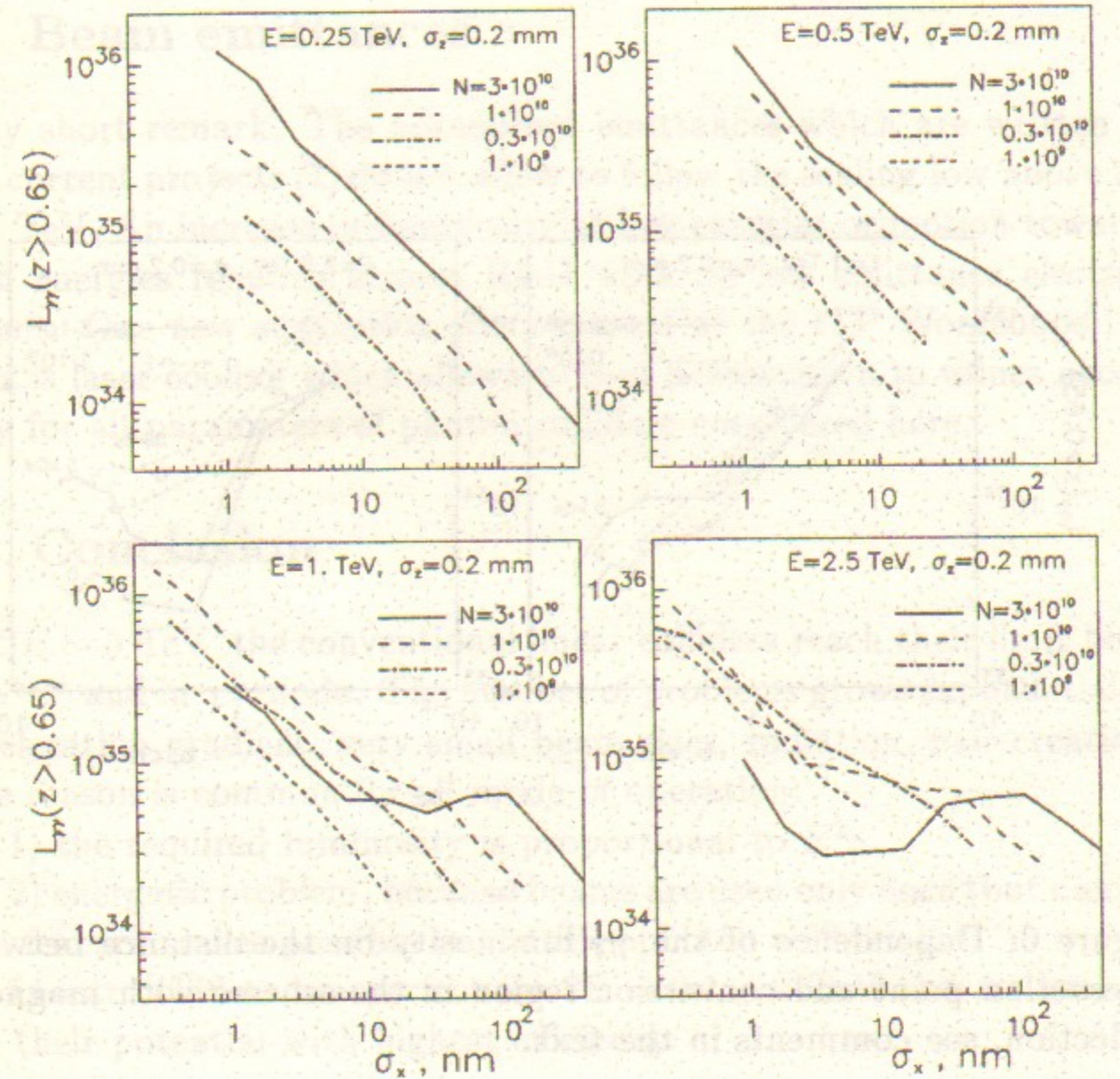


Figure 5: Dependence of the $\gamma\gamma$ luminosity on the horizontal beam size for $\sigma_z = 0.2 \text{ mm}$, see comments in the text.

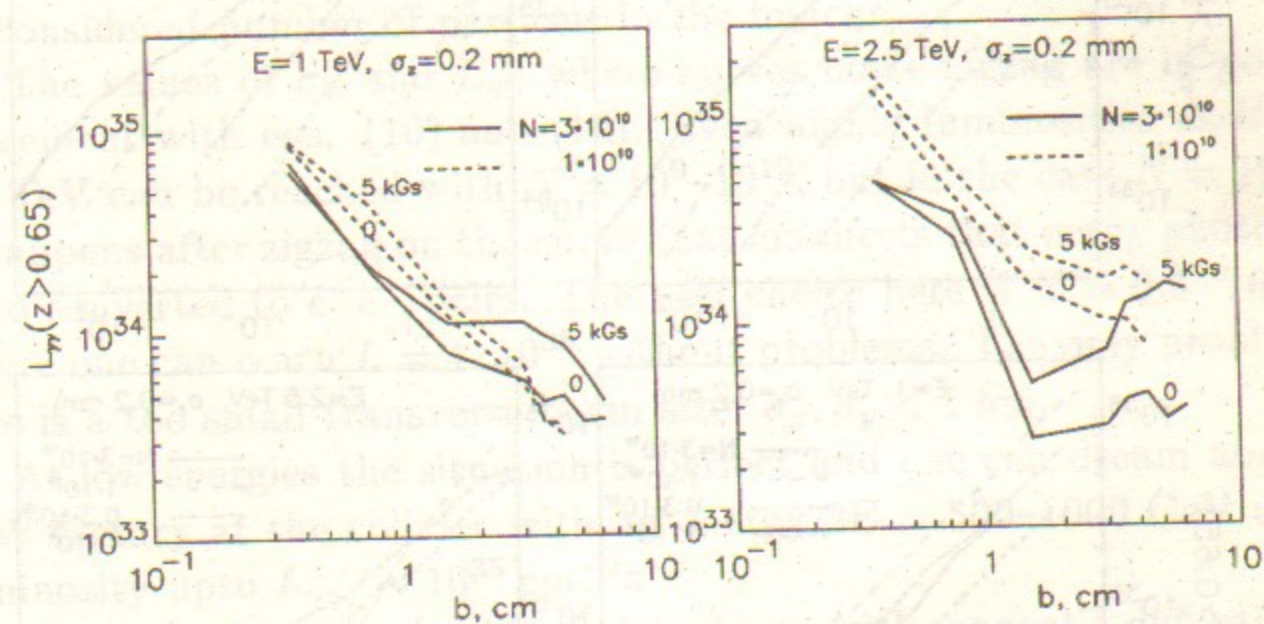


Figure 6: Dependence of the $\gamma\gamma$ luminosity on the distance between interaction point and conversion region in the scheme with magnetic deflection, see comments in the text.

problems for the required average laser power. It seems that $f=10-30$ kHz is still acceptable. With $N=0.3 \cdot 10^{10}$ one can reach at $2E=5$ TeV even a few times higher luminosity than that it is 'required'. The main problem here is connected with attainable beam emittances.

7 Beam emittances

Only short remark. The normalized emittances which are written in the current projects [1] do not allow to follow the scaling law above $2E = 1$ TeV. An increase in luminosity at low energies or motion towards high energies requires serious R&D work on low emittance electron beams. One new suggestion was reported at the ITP Workshops[10]. This is laser cooling which allows to cool beams down to values necessary for all parameters of photon colliders considered here.

8 Conclusion

At $2E \sim 5$ TeV the conventional linear colliders reach their limit both in e^+e^- and in $\gamma\gamma$ mode. The number of problems grows exponentially: acceleration gradient, very small beam sizes, radiation, pair creation. The reason is common for all mode of operation:

- 1) the required luminosity is proportional to E^2 ;
- 2) energetic problem, because beams are used only once (but namely this feature makes possible to consider photon colliders).

Linear colliders are perfect for $2E = 0.1 - 2$ TeV and we have to use their potential with highest efficiency.

Acknowledgments

I would like to thank Z.Parza, the organizer of the Program "New Ideas for Particle Accelerator" at ITP, UCSB, Santa Barbara, supported with National Science Foundation Grant NO PHY94-07194.

References

- [1] Low et al., International Linear Collider Technical Review Committee Report, SLAC-Rep-471(1996)
- [2] I.Ginzburg, G.Kotkin, V.Serbo, V.Telnov, *Pizma ZhETF*, **34** (1981)514; *JETP Lett.* **34** (1982)491.
- [3] I.Ginzburg, G.Kotkin, V.Serbo, V.Telnov, *Nucl.Instr. & Meth.* **205** (1983) 47.
- [4] V.Telnov, *Nucl.Instr.&Meth.A* **294** (1990)72.
- [5] V.Telnov, *Nucl.Instr.&Meth.A* **355**(1995)3.
- [6] *Proc.of Workshop on $\gamma\gamma$ Colliders*, Berkeley CA, USA, 1994, *Nucl. Instr. &Meth. A* **355**(1995)1-194.
- [7] P.Chen, V.Telnov, *Phys.Rev.Letters*, **63** (1989)1796.
- [8] V.Telnov, *Proc.of Workshop 'Photon 95'*, Sheffield, UK, April 1995, p.369.
- [9] *Zeroth-Order Design Report for the Next Linear Collider* LBNL-PUB-5424, SLAC Report 474, May 1996.
- [10] V.Telnov, *Proc.of ITP Workshop 'New modes of particle accelerations techniques and sources* Santa Barbara, USA, August 1996, NSF-ITP-96-142, SLAC-PUB 7337, e-print hep-ex/9610008.

V.I. Telnov

Ultimate luminosities and energies of photon colliders

В.И. Тельнов

Предельная светимость и энергия фотонных коллайдеров

Budker INP 97-47

Ответственный за выпуск А.М. Кудрявцев
Работа поступила 4.06.1997 г.

Сдано в набор 8.06.1997 г.

Подписано в печать 4.06.1997 г.

Формат бумаги 60×90 1/16 Объем 1.0 печ.л., 0.9 уч.-изд.л.

Тираж 150 экз. Бесплатно. Заказ N 47.

Обработано на IBM PC и отпечатано на
ротапинтере ГНЦ РФ "ИЯФ им. Г.И. Будкера СО РАН",
Новосибирск, 630090, пр. академика Лаврентьева, 11.